

Effect of new Curcumin-containing nanostructured lipid dispersions on human keratinocytes proliferative responses

Journal:	<i>Experimental Dermatology</i>
Manuscript ID:	EXD-14-0473
Manuscript Type:	Regular Article
Date Submitted by the Author:	20-Oct-2014
Complete List of Authors:	Esposito, Elisabetta; University of Ferrara, Life Sciences and Biotechnology Sticozzi, Claudia; University of Ferrara, Life Sciences and Biotechnology Ravani, Laura; University of Ferrara, Life Sciences and Biotechnology Drechsler, Markus Muresan, Ximena; University of Ferrara, Life Sciences and Biotechnology Cervellati, Franco; University of Ferrara, Life Sciences and Biotechnology Cortesi, Rita; University of Ferrara, Life Sciences and Biotechnology Valacchi, Giuseppe; University of Ferrara,
Keywords:	Curcumin, Nanoparticles, NFkB, Cyclin D1, Keratinocytes

1
2
3
4
5
6
7
8
9
10
11
12
13
14
15
16
17
18
19
20
21
22
23
24
25
26
27
28
29
30
31
32
33
34
35
36
37
38
39
40
41
42
43
44
45
46
47
48
49
50
51
52
53
54
55
56
57
58
59
60

1 **Effect of new Curcumin-containing nanostructured lipid dispersions on human keratinocytes**
2 **proliferative responses.**

3 Elisabetta Esposito^{a#}, Claudia Sticozzi^{a#}, Laura Ravani^a, Markus Drechsler^b, Ximena M Muresan^a,
4 Franco Cervellati^a, Rita Cortesi^a, Giuseppe Valacchi^{a*}

5
6 ^a*Department of Life Sciences and Biotechnology, Section of Medicinal and Health Products,*
7 *University of Ferrara, I-44121 Ferrara, Italy*

8 ^b*Macromolecular Chemistry II, University of Bayreuth, Germany*

9
10 # Equally contributed to the study

11
12 *Correspondence to:

13 Giuseppe Valacchi, PhD
14 Department of Life Sciences and Biotechnology,
15 University of Ferrara,
16 44121 Ferrara, Italy
17 (39) 0532 455 482
18 giuseppe.valacchi@unife.it
19

20
21

22 Abstract

23 The present study describes the production and characterization of nanostructured lipid dispersions
24 (NLD) containing curcumin (CUR) as new tools for curcumin topical delivery.

25 Four types of NLD based on monoolein in association with different emulsifiers were produced: Na
26 cholate and poloxamer 407 (NLD1), poloxamer alone (NLD2), the mixture of Na cholate and Na
27 caseinate (NLD3) and Na cholate alone (NLD4). Morphology, dimensional distribution of lipid
28 dispersions were investigated by cryo-TEM and Photon Correlation Spectroscopy (PCS). In vitro
29 studies based on Franz cell and membrane nylon, and stratum corneum-epidermis (SCE) were
30 carried out in order to compare CUR diffusion from selected lipid dispersions. In addition the NLDs
31 cytotoxicity was evaluated in human keratinocytes.

32 PCS studies showed differences in particles diameter among the different NLDs. Cytotoxicity
33 results in HaCaT cells evidenced that NLD1 and NLD2 were toxic at doses over 1 μ M. Therefore
34 Cryo-TEM was determined only for NLD3 and NLD4 showing the unilamellar vesicles without
35 any effect on the structure by CUR. Diffusion measurement in SCE and nylon membrane evidenced
36 that CUR had a time delayed release for NLD4. The “wound healing” effect of NLD3 and NLD4
37 with and without CUR was analysed keratinocytes in vitro. Results showed a clear inhibition of cell
38 proliferation/migration by CUR. This effect was mediated by the inhibition of cyclin D1 expression
39 as a consequence of the impaired NFkB activation.

40 This study confirms the antiproliferative properties of CUR and evidenced a new possible model of
41 CUR topical delivery for hyperproliferative cutaneous diseases such as psoriasis.

42
43 *Keywords:* cubosomes, curcumin, HaCaT, cyclinD1, NFkB

44
45 Abbreviations: Nanostructured lipid dispersions (NLD); curcumin (CUR); Cryogenic Transmission
46 Electron Microscopy (cryo-TEM), Photon Correlation Spectroscopy (PCS) stratum corneum-
47 epidermis (SCE).

1
2
3
4
5
6
7
8
9
10
11
12
13
14
15
16
17
18
19
20
21
22
23
24
25
26
27
28
29
30
31
32
33
34
35
36
37
38
39
40
41
42
43
44
45
46
47
48
49
50
51
52
53
54
55
56
57
58
59
60

48

For Review Only

49 1. Introduction

50 Curcumin (CUR) is a polyphenol derived from the spice turmeric, with an age-old tradition as a
51 drug [1, 2]. Among its numerous activities, CUR is able to affect skin proliferative properties by
52 modulating the expression of growth related proteins [1, 2]. Despite its efficacy, CUR is scarcely
53 soluble in water and in particular it is not readily absorbed through the skin, hence arduous to be
54 administered.

55 At this regard many delivery strategies for CUR have been proposed, mainly based on the use of
56 lipid matrixes such as liposomes, solid lipid nanoparticles, and cyclodextrins [3, 4]. In particular
57 our group has proposed the solubilization of CUR in nanostructured lipid dispersions (NLD) [5, 6].

58 Lipid dispersions enable to gain dissolution and controlled delivery of active molecules, at the same
59 time improving drug bioavailability and reducing side-effects [7, 8]. The emulsification of
60 unsaturated long-chain monoglycerides in water in the presence of an emulsifier results in the
61 formation of aqueous nanostructured dispersions with a complex disperse phase based on lyotropic
62 liquid crystalline phases (lamellar, hexagonal, and cubic) [9, 10]. The emulsifier exerts an important
63 role since it influences both structure and stability of the disperse phase [6, 11].

64 In the present investigation four NLD based on monoolein in association with different emulsifiers
65 and loaded with CUR have been produced and characterized with the aim to obtain new tools to
66 possibly modulate keratinocytes proliferation.

67 Morphology and dimensional distribution of NLDs have been investigated by Cryogenic
68 Transmission Electron Microscopy (cryo-TEM) and Photon Correlation Spectroscopy (PCS).

69 The permeability of CUR from NLDs has been investigated by Franz cell alternatively associated to
70 stratum corneum-epidermis (SCE) or nylon membranes. The latest have been chosen in order to
71 simulate cutaneous tissue. In our studies we were able to evidence that CUR did not affect the
72 diameter and the structure of the particles (NLDs). “In vitro” study showed that a slight cytotoxicity
73 of NLD1 and NLD2; while, CUR loaded in NLD3 and NLD4 was able to affect cell proliferation by

1
2
3
4
5
6
7
8
9
10
11
12
13
14
15
16
17
18
19
20
21
22
23
24
25
26
27
28
29
30
31
32
33
34
35
36
37
38
39
40
41
42
43
44
45
46
47
48
49
50
51
52
53
54
55
56
57
58
59
60

74 inhibiting the activation of NFkB/cyclin D1 pathway, suggesting a possible new toll for CUR
75 delivery.
76

For Review Only

77 2. Methods

78 2.1 Materials

79 Glyceryl monooleate RYLO MG 19 (monoolein) was a gift from Danisco Cultor (Grindsted,
80 Denmark). Pluronic F127 (Poloxamer 407, poloxamer) (PEO₉₈-POP₆₇-PEO₉₈) was obtained from
81 BASF (Ludwigshafen, Germany). Curcumin (CUR), (1E,6E)-1,7-bis(4-Hydroxy-3-
82 methoxyphenyl)-1,6-heptadiene-3,5-dione, sodium cholate (Na cholate) (3 α ,7 α ,12 α -Trihydroxy-5 β -
83 cholanyl-24-oic acid sodium salt), and sodium caseinate (Na caseinate) (α S1, α S2, β , κ) were
84 purchased from Sigma Chemical Company (St Louis, MO, USA). Solvents were of HPLC grade
85 and all other chemicals were of analytical grade.

87 2.2. NLD preparation

88 Production of dispersions was based on the emulsification of monoolein and emulsifier in water, as
89 previously described [5, 6]. NLD compositions are reported in Table I.

90 After emulsification, the dispersions were subjected to homogenization (15,000 rev min⁻¹, Ultra
91 Turrax, Janke & Kunkel, Ika-Werk, Sardo, Italy) at 60°C for 1 min, then cooled and maintained at
92 room temperature in glass vials.

93 To produce CUR containing NLD (CUR-NLD), 7.5 mg of CUR (0.33% w/w with respect to the
94 monoolein, 0.015% w/w with respect to the dispersion) were added to the molten
95 monoolein/emulsifier mixture and dissolved before addition to the aqueous solution. During
96 production the vial was protected from light with an aluminium foil to prevent photo-degradation of
97 CUR.

99 2.2 Characterization of NLD

100 2.2.1 Cryo-Transmission Electron Microscopy (Cryo-TEM)

101 Samples were vitrified as described in a previous study [6, 12]. The vitrified specimen was
102 transferred to a Zeiss EM922Omega (Carl Zeiss Microscopy, Oberkochen, Germany) transmission

1
2
3 103 electron microscope using a cryoholder (CT3500, Gatan, Munich, Germany). Sample temperature
4
5 104 was kept below 100K throughout the examination. Specimens were examined with reduced doses of
6
7 105 about 1000-2000 e/nm² at 200 kV. Images were recorded by a CCD digital camera (Ultrascan 1000,
8
9 106 Gatan, Munich, Germany) and analysed using a GMS 1.8 software (Gatan, Munich, Germany).

107 108 2.2.2 Photon Correlation Spectroscopy (PCS)

109 Submicron particle size analysis was performed using a Zetasizer 3000 PCS (Malvern Instr.,
110 Malvern, England) equipped with a 5 mW helium neon laser with a wavelength output of 633 nm.
111 Glassware was cleaned of dust by washing with detergent and rinsing twice with sterile water.
112 Measurements were made at 25 °C at an angle of 90° with a run time of at least 180 sec. Samples
113 were diluted with bidistilled water in a 1:10 v:v ratio. Data were analysed using the “CONTIN”
114 method [13]. Measurements were performed on NLD after production.

115 116 2.3. *In vitro* diffusion studies

117 In vitro diffusion studies were performed by Franz type diffusion cells supplied by LGA (Berkeley,
118 CA) associated to SCE or nylon membranes (Millipore, 0.45 μm pore size).

119 Samples of adult human skin (mean age 36±8 years) were obtained from breast reduction operations
120 and treated as previously reported [6, 8, 14].

121 Samples of dried SCE or nylon membranes were rehydrated by immersion in distilled water at room
122 temperature for 1 h before being mounted in Franz cell. The exposed skin surface area was 0.78 cm²
123 (the diameter of the orifice was 1 cm). The receptor compartment contained 5 ml of a mixture of
124 phosphate buffer 60 mM pH 7.4 and methanol (50:50, v/v) as above reported. This solution was
125 stirred with the help of a magnetic bar at 500 rpm and thermostated at 32 ± 1°C during all the
126 experiments [15].

127 Approximately 500 μl of each formulation was placed on the skin surface in the donor compartment
128 and the latter was sealed to avoid evaporation. At predetermined time intervals comprised between

1
2
3 129 1 and 24 hours, samples (0.15 ml) of receptor phase were withdrawn and CR concentration in the
4
5 130 receptor phase was measured using HPLC. Each removed sample was replaced with an equal
6
7 131 volume of simple receptor phase. The CUR concentrations were determined six times in
8
9 132 independent experiments and the mean values \pm standard deviations were calculated. The mean
10
11 133 values were then plotted as a function of time. The diffusion coefficients, computed from the linear
12
13 134 portion of the accumulation curve, represent the experimentally observed fluxes (F_o).

15
16 135 Normalized fluxes F_n were then calculated by the following equation:

17
18 136
$$F_n = F_o/C \quad (1)$$

19
20 137 where C is the CUR concentration (in mg/ml) in the analysed form.

21
22 138

23 24 139 *2.4 HPLC Procedure*

25
26 140 HPLC determinations were performed using a two-plungers alternative pump (Jasco, Japan), an
27
28 141 UV-detector operating at 425 nm, and a 7125 Rheodyne injection valve with a 50 μ l loop. Samples
29
30 142 were loaded on a stainless steel C-18 reverse-phase column (15 \times 0.46 cm) packed with 5 μ m
31
32 143 particles (Grace[®] - Alltima, Alltech, USA).

33
34 144 Elution was performed with a mobile phase containing methanol, 2% acetic acid and acetonitrile
35
36 145 5:30:65 v/v at a flow rate of 0.5 ml/min. Retention time of CUR was 7.0 min.

37
38 146

39 40 147 *2.5 Cell culture and treatments*

41
42 148 HaCaT cells, (a cell line gift from Dr. F. Virgili), were grown in Dulbecco's modified Eagle's
43
44 149 medium High Glucose (Lonza, Milan, Italy), supplemented with 10% FBS, 100 U/ml penicillin,
45
46 150 100 μ g/ml streptomycin and 2 mM l-glutamine as previously described [16]. Cell suspension
47
48 151 containing 10 or 1×10^5 viable cells/ml were used. Cells were incubated at 37 $^{\circ}$ C for 24 h in 95%
49
50 152 air/5% CO₂ until 80% confluency.

51
52 153 HaCaT cells were treated with different doses of these preparations (1 and 10 nM) at different time
53
54 154 points (1 and 24 h).

1
2
3 155 After treatment, cells or medium were collected for the several assays described below.
4
5 156 CUR were dissolved in ETOH at a concentration of 10 mM as a stock solution. The stock was
6
7 157 diluted to the required concentrations directly in the medium. The final concentration of ETOH in
8
9 158 culture medium during compounds treatment did not exceed 0.1% (v/v).
10
11
12 159

13 160 *2.6 Cellular viability*

14
15
16 161 Viability studies were performed 24 h after treatments by cytofluorimetric (Muse Cell Analyzer)
17
18 162 and LDH release assay. The cytofluorimetric assay was performed by using Muse Count & Viability
19
20 163 Kit (Millipore, Corporation, Billerica, MA, USA). Briefly, 380 μ L of Muse Count&Viability
21
22 164 working solution were added to cells (1×10^6 cell/mL), and 20 μ L of this cell suspension were
23
24 165 incubated for 5 minutes at room temperature in the dark.
25
26

27 166 In addition, the LDH release was measured by enzymatic assay: in the first step NAD^+ is reduced
28
29 167 to NADH/H^+ by the LDH-catalyzed conversion of lactate to pyruvate; in the second step the
30
31 168 catalyst (diaphorase) transfers H/H^+ from NADH/H^+ to tetrazolium salt which is reduced to
32
33 169 formazan. Prior to each assay, the cells were lysed with 2% (V/V) Triton X-100 in culture media for
34
35 170 30 min at 37 °C to obtain a representative maximal LDH release as the positive control with 100%
36
37 171 toxicity The amounts of LDH in the supernatant were determined and calculated according to kit
38
39 172 instructions (EuroClone Milan, Italy). All tests were performed in triplicate repeated at least three
40
41 173 times.
42
43
44

45 174

46 47 175 *2.8 Wound healing "in vitro" assay*

48
49 176 HaCaT cells (2×10^6 per well) were seeded in a 60×15 mm Petri dishes and grown until confluent.
50
51 177 Cells were then treated with CUR, CUR-NLD3 and CUR-NLD4 (1 and 10nM) for 24 h. Each
52
53 178 monolayer was scratched with the use of a 200 μ l pipette tip to generate a cell-free zone (0.8–1 mm
54
55 179 in width). After washing with DMEM, cells were incubated for 24 h at 37°C with DMEM 10%
56
57 180 FBS. Cells were photographed 1hrs after wounding, the wounded area was marked on the base of
58
59
60

1
2
3 181 the Petri dish, and the same field was photographed again after incubation for 24 h. The migration
4
5 182 of cells into the wound area was evaluated. Images were acquired on a Leica imaging microscope.
6

7 183

8
9 184 *2.9 Western blot analysis*

10 185 After protein extraction in RIPA buffer, 60 µg boiled protein were loaded onto 10% sodium dodecyl
11
12 186 sulphate–polyacrylamide electrophoresis gels and separated by molecular size. Gels were electro-
13
14 187 blotted onto nitrocellulose membranes and then blocked for 1 h in Tris-buffered saline, pH 7.5,
15
16 188 containing 0.5% Tween20 and 5% milk. Membranes were incubated overnight at 4 °C with the
17
18 189 rabbit anti- cyclin D1 (Millipore Corporation, Billerica, MA, USA [clone EPR 224 (IHC)-32]) or β-
19
20 190 actin (Millipore Corporation, Billerica, MA, USA). The membranes were then incubated with
21
22 191 horseradish peroxidase-conjugated secondary antibody (anti-rabbit) for 1 h, and the bound
23
24 192 antibodies were detected by chemiluminescence (BioRad, Milan, Italy). β-Actin was used as
25
26 193 loading control. Images of the bands were digitized and the densitometry analysis was performed
27
28 194 using Image-J software.
29
30
31
32
33

34 195

35
36 196 *2.10 Immunocytochemistry*

37
38 197 Briefly, HaCaT cells were grown on coverslips in medium with FBS 10%, at a density of 1×10^5
39
40 198 cell/ml, and after treatments were fixed in 4% paraformaldehyde in PBS for 30 min at 4 °C. Cells
41
42 199 were permeabilized and then blocked in PBS containing 5% BSA at RT for 1 h. Coverslips were
43
44 200 then incubated for 1 h with primary antibody (anti p65 subunit, SantaCruz, CA), followed by 1 h
45
46 201 with secondary antibodies. Nuclei were stained with 1 µg/ml DAPI (Molecular Probes) for 1 min
47
48 202 after removal of secondary antibodies. Coverslips were mounted onto glass slides using with anti-
49
50 203 fade mounting medium 1,4-diazabicyclo[2.2.2]octane in glycerine (DABCO) and examined by the
51
52 204 Leica light microscope equipped with epifluorescence at 63X magnification. Negative controls were
53
54 205 performed by omitting primary antibodies.
55
56
57
58
59
60

1
2
3
4
5
6
7
8
9
10
11
12
13
14
15
16
17
18
19
20
21
22
23
24
25
26
27
28
29
30
31
32
33
34
35
36
37
38
39
40
41
42
43
44
45
46
47
48
49
50
51
52
53
54
55
56
57
58
59
60

206 *Statistical Analysis*

207 For each of the variables tested, two-way analysis of variance (ANOVA) was used. A significant
208 effect was indicated by a *P*-value < 0.05. Data are expressed as mean ± S.D. of triplicate
209 determinations obtained in 5 independent experiments.

210

211

For Review Only

212 3. Results

213 3.1 Preparation and characterization of NLD

214 In the present study we have studied the cytotoxicity of four different NLD obtained in the presence
215 of (a) Na cholate and poloxamer 407 (NLD 1), (b) poloxamer alone (NLD 2), (c) the mixture of Na
216 cholate and Na caseinate (NLD3) and (d) Na cholate alone (NLD4), (see Table I).

217 PCS studies were conducted to determine the dimensional distribution of NLD, in the absence and
218 in the presence of CUR. Table II summarizes the obtained results expressed as intensity mean
219 diameter and polydispersity index (P.I.). It can be observed that the mean diameter of the NLD
220 disperse phase after production is comprised between 150 and 230 nm. The lowest diameter was
221 obtained by the use of Na cholate and poloxamer 407 while the highest in the case of Na cholate
222 and Na caseinate. P.I. was not affected by the employed surfactant.

223

224 3.2 Cytotoxicity studies

225 Cytotoxicity of CUR-NLDs ranging from 1 to 100 nM was evaluated in HaCaT cells by means of
226 cytofluorimetric assay and LDH release. Treatment for 24hrs with NLD1 and NLD2, induced
227 cytotoxic effect (data not shown), while, NLD3 and NLD4 treatment did not affect cell viability as
228 it is shown in Fig. 1A. These results were in line with the LDH release. In fact, as it is depicted in
229 Fig. 1B, treatment with NLD3 and NLD4 did not induce the release of LDH in the media.

230

231 3.3 CUR containing NLD

232 The cytotoxicity study enabled to select NLD3 and NLD4 as the less toxic nano-dispersions to be
233 employed for keratinocytes studies. To this aim NLD were produced in the presence of CUR (CUR-
234 NLDs) and characterized in term of size and morphology.

235 Concerning dimensions, from data reported in Table III, it should be noted that the mean diameter
236 of NLD disperse phase is not affected by the presence of CUR.

1
2
3 237 Cryo-TEM analyses were conducted in order to investigate the internal structures of NLDs and to
4
5 238 compare the influence of the emulsifier on the nanostructure of the dispersed phase. Figure 2 reports
6
7 239 cryo-TEM images of NLD3 (panels A and B) and CUR- NLD3 (panels C and D). All panels show
8
9 240 mixtures of vesicles, cubosomes and hexasomes. In particular, in Figure 2A mainly unilamellar
10
11 241 vesicles can be observed together with invaginated ones. Figure 2B shows a particle with the typical
12
13 242 inner cubic structure. In both Figures 2C and 2D some hexasomes in different formation state are
14
15 243 reported, besides plain vesicles and vesicles with invaginations. The amphiphilic protein casein,
16
17 244 exhibits self-association into micellar aggregates in water and it is able to form cubosomes in the
18
19 245 presence of monoolein, as previously demonstrated by other authors [17, 18]. CUR does not
20
21 246 influence NLD disperse phase.
22
23

24
25 247 The morphology of NLD4 and CUR- NLD4, whose cryo-TEM images are respectively reported in
26
27 248 Fig. 3A and 3B, was characterized by unilamellar vesicles. The black dots are ascribed to ice
28
29 249 crystals contamination due to sample preparation. Also in this case the presence of CUR does not
30
31 250 seem to affect NLD aspect.
32
33

34 251

35 252 *3.4. CUR permeability study*

36
37 253 Franz cell was employed to compare the diffusion kinetics of CUR from CUR-NLD3 and CUR-
38
39 254 NLD4. SCE and nylon membranes were employed and their performances were compared.
40
41

42
43 255 A non-physiological receptor phase with 50% v/v of ethanol was used, in order to allow the
44
45 256 establishment of the sink conditions and to sustain permeant solubilization [8, 19]. Figure 4
46
47 257 summarizes the results obtained by SCE (panel A) and nylon (panel B) membranes.
48

49
50 258 CUR-NLD4 resulted in the fastest diffusion of the drug both in the case of SCE and nylon
51
52 259 membranes. The differences between the CUR diffusion data were extremely significant
53
54 260 ($p < 0.0001$).
55

56
57 261 The slope, which represents the release rate, steady-state flux, was calculated by linear regression of
58
59 262 the linear portion of the curve. In the case of SCE membrane the CUR calculated fluxes from NLD3
60

1
2
3 263 and NLD4 were 0.093 and 0.22×10^{-3} cm/h respectively, while by the use of nylon membrane the
4
5 264 fluxes were 9.24 and 42.93×10^{-3} cm/h for NLD3 and NLD4 respectively. Hence CUR diffuses
6
7 265 more slowly from NLD3 than from NLD4.
8

9
10 266 The CUR fluxes obtained by nylon were about 200 fold higher than those obtained by SCE, this
11
12 267 result was expectable since SCE porosity is about 80 nm while nylon membrane displays a porosity
13
14 268 of 450 nm.
15

16 269

17 270 *3.5. Wound healing study*

18
19
20 271 Since it is well known that CUR is a natural compound with anti-proliferative effect on several cell
21
22 272 type, we have examined the impact of NLDs plus CUR in an “in vitro” scratch wound model. As it
23
24 273 is shown in Fig. 5, CUR-NLDs hampered the ability of HaCaT cells to regenerate the monolayer in
25
26 274 the scratched area, resulting in a delayed closure of the wound. In the specific, NLD4+CUR (1 and
27
28 275 10nM) was able to significantly delay the wound closure already after 20hr from the “scratch” (
29
30 276 33%). This effect was also noticed for NLD3+CUR (10nM) although it was less evident and
31
32 277 reached the significance only at 24h. No differences were noticed respect to NLDs when the cells
33
34 278 were treated with the only CUR (data not shown).
35
36 279

37 280 *3.6 Cyclin D1 expression*

38
39
40 281 As shown in Fig. 5, CUR treatment was able to reduced the expression of Cyclin D1 in a dose
41
42 282 dependent manner after 24 hr of treatment (20% for 1nM and 70% for 10 nM). Similar results were
43
44 283 observed when the cells were treated with NLD3+CUR (1 and 10nM). On the contrary, only 10nM
45
46 284 NLD4+CUR were able to significantly affect Cyclin D1 protein levels (57%).
47
48
49
50

51 285

52 286 *3.7 NFkB nuclear translocation study*

53
54
55 287 Being Cyclin D1 under the control of the transcription factor NFkB, we have evaluated the
56
57 288 activation (nuclear translocation) of this transcription factor. As shown in Fig. 7, 1h after the
58
59
60

1
2
3
4
5
6
7
8
9
10
11
12
13
14
15
16
17
18
19
20
21
22
23
24
25
26
27
28
29
30
31
32
33
34
35
36
37
38
39
40
41
42
43
44
45
46
47
48
49
50
51
52
53
54
55
56
57
58
59
60

289 treatment of the cells with 1 and 10 nM of CUR, there was an evident decrease in NFkB activation
290 (green color) as measured by its nuclear translocation. Similar effect was observed when the cells
291 were treated with sodium NLD4 (1 and 10nM) and NLD3 (10 nM) and these data parallel with the
292 Cyclin D1 results.
293

For Review Only

1
2
3 294 **Discussion**

4
5 295 In the current paper we demonstrate that NLDs-CUR are a strong inhibitors of keratinocytes
6
7 296 proliferation. Because keratinocytes abnormal proliferation in psoriatic skin mimics an overshoot
8
9 297 wound-healing process, we tested the potential effect of NLDs-CUR in an “in vitro” scratch wound
10
11 298 model. We found that CUR hampered the monolayer reconstitution in the wound site, markedly
12
13 299 delaying spontaneous wound closure. Further work is needed to assess whether NLDs-CUR impaire
14
15 300 wound healing by simply blocking cell proliferation or, additionally, by decreasing cell motility.

16
17
18 301 CUR is a component of turmeric and it has been used, for first time, as a medical remedy in
19
20 302 Southeast Asia for centuries. This compound, in fact, has different properties including antioxidant,
21
22 303 anti-carcinogenic, anti-viral, and anti-infectious as well as anti-inflammatory and anti- proliferative
23
24 304 activity [20–22]. Many of CUR functions have been attributed to its ability to modulate
25
26 305 transcription factors and lots of work has been done on the effect of CUR on NFkB [23, 24].
27
28 306 Several papers have now evidenced the ability of CUR to inhibit the activation of NFkB and
29
30 307 therefore to regulate several cellular processes among which cellular proliferation is a key
31
32 308 component in cutaneous tissues. Indeed, cellular proliferation and differentiation are tightly
33
34 309 regulated in skin and their alteration can lead to several pathologies. For instance, psoriasis is
35
36 310 characterized by hyper-proliferative and altered differentiation of keratinocytes [25]. Several natural
37
38 311 products have been investigated to ameliorate or cure psoriasis and CUR has been extensively
39
40 312 studied in cutaneous tissues where can be applied topically.

41
42
43 313 Although the numerous beneficial properties, CUR molecule is not easily absorbed through the
44
45 314 skin. Therefore the aim of this study was to produce and characterize NLDs containing CUR as new
46
47 315 tools for its topical delivery.

48
49
50 316 It is well known that the emulsification of monoolein in water in the presence of a surfactant such as
51
52 317 poloxamer 407 leads to the production of cubosome dispersions [10, 26, 27]. Some authors have
53
54 318 found a moderate toxicity toward blood components exhibited by cubosomes stabilized by
55
56 319 poloxamer 407 [28] due to the synergistic action of poloxamer 407 and monoolein. The produced
57
58
59
60

1
2
3 320 nanostructures would be able to exert a very low but detectable hemolytic activity. To possibly
4
5 321 overcome this drawback we have produced and characterized heterogeneous monoolein dispersions
6
7 322 by the use of alternative emulsifiers such as Na cholate and Na caseinate [5, 6]. We found that the
8
9 323 mean diameter of the NLD disperse phase after production is comprised between 150 and 230 nm.
10
11 324 The lowest diameter was obtained by the use of Na cholate and poloxamer 407 while the highest in
12
13 325 the case of Na cholate and Na caseinate. P.I. was not affected by the employed surfactant. In
14
15 326 addition loading the NLDs with CUR did not affect the size and the properties of the nanostructured
16
17 327 lipids.

18
19
20 328 Concerning the membranes for Franz diffusion studies, excised human or animal skin can be
21
22 329 preferably used in order to obtain reliable permeability results [29]. Nonetheless, synthetic
23
24 330 membranes can also be employed when biological skin is not readily available [30]. Synthetic
25
26 331 membranes should have minimum diffusion resistance to drugs and only act as a support to separate
27
28 332 the formulation from the receptor medium, in this respect in the present study SCE was chosen to
29
30 333 reproduce the human skin, while nylon was employed to simulate the cutaneous wounds, where the
31
32 334 skin is not continuous and integer but is damaged instead. In any case CUR diffusion appears fastest
33
34 335 by the use of NLD4. In this regards the different inner morphology NLD should be considered: the
35
36 336 disperse phase of NLD3 is constituted of a mixture of well organized structures such as cubosomes,
37
38 337 hexasomes and different types of vesicles, while NLD4 disperse phase is mainly based on vesicles.
39
40
41
42 338 Hence it is conceivable that CUR transition through NLD4 is more easy than through NLD3, where
43
44 339 the different supramolecular structures perplex the CUR passage, at last leading to a slower
45
46 340 diffusion.

47
48
49 341 In addition our results demonstrated that NLD3 and NLD4, did not have any toxic effect in human
50
51 342 keratinocytets and especially for NLD4 there was a significant delay in cell proliferation by the use
52
53 343 of an in vitro scratch wound model. This effect could be the consequence of the inhibition of NFkB
54
55 344 activation that subsequently affect Cyclin D1 expression.
56
57
58
59
60

1
2
3 345 Skin injury activated a number of signaling pathways that induce the increased cell proliferation,
4
5 346 resulting in the formation of scar tissue. These pathways are mediated by the transcription regulator
6
7 347 NFkB. Prior to injury, NFkB exists as a pair of dimers (p50/p65) within the cytoplasm. When
8
9 348 activated by a number of inflammatory stimuli, including surgical injury, NFkB dimers translocate
10
11 349 into nucleus, where they bind to DNA, and induce the transcription of over 200 genes responsible
12
13 350 for cell proliferation, cell migration, cell cycling, and the inhibition of apoptosis [31-33].

14
15 351 The activation of NF-kB requires phosphorylation at multiple serine/threonine-specific sites as well
16
17 352 as tyrosinespecific sites [33, 36]. The process of activating NFkB requires the removal of its
18
19 353 inhibitory protein, Ikb, by phosphorylation of its kinase, Ikb kinase. Ikb kinase is a
20
21 354 serine/threonine kinase which is activated by PhK. It has been demonstrated that PhK is inhibited
22
23 355 by CUR [37].

24
25 356 Therefore it is possible to hypothesize that CUR-NLDs are capable of penetrating injured skin, such
26
27 357 as in psoriasis, sufficiently to decrease adenosine triphosphate (ATP)-phosphorylase b
28
29 358 phosphotransferase PhK levels within the epidermis. These data are in agreement with the study of
30
31 359 Heng et al. [38] that demonstrated that CUR gel is also capable of penetrating at least as far as the
32
33 360 superficial dermis in post-surgical scars, with significant resolution of post-surgical scarring. Our
34
35 361 data support the fact that NLDs could be a good alternative of delivering “beneficial” molecules to
36
37 362 the skin ameliorating the ability to be absorbed thank also to the slow time release. In this specific
38
39 363 case, NLD4 seems to release CUR faster than NLD3 showing even a lower cellular toxicity. These
40
41 364 molecules could be also used not only for hyper-proliferative diseases but, as it has shown in the
42
43 365 work by Heng et al., also to optimize the time of wound-closure to avoid the formations of scars
44
45 366 [38]. In conclusion NLDs are a new and promising tool to ameliorate the pathogenesis of several
46
47 367 skin diseases thanks to the possibility to apply them topically.
48
49
50
51
52
53
54
55
56
57
58
59
60

371 **References**

372

373 [1] Aggarwal B B, Harikumar K B. Potential therapeutic effects of curcumin, the anti-inflammatory
374 agent, against neurodegenerative, cardiovascular, pulmonary, metabolic, autoimmune and
375 neoplastic diseases. *Int J Biochem Cell Biol* 2009; 41: 40-59.

376

377 [2] Thangapazham R L, Sharma A, Maheshwari R K. Beneficial role of curcumin in skin diseases.
378 *Adv Exp Med Biol* 2007; 595: 343-357.

379

380 [3] Bhawana B, Basniwal R K, Buttar H S, *et al.* Curcumin nanoparticles: preparation,
381 characterization, and antimicrobial study. *J Agric Food Chem* 2011; 59: 2056-2061.

382

383 [4] Tonnesen H H, Masson M, Loftsson T. Studies of curcumin and curcuminoids. XXVII.
384 Cyclodextrin complexation: solubility, chemical and photochemical stability. *Int J Pharm* 2002;
385 244: 127-135.

386

387 [5] Puglia C, Cardile V, Panico A M, *et al.* Evaluation of monooleine aqueous dispersions as tools
388 for topical administration of curcumin: characterization, in vitro and ex-vivo studies. *J Pharm Sci*
389 2013; 102: 2349-2361.

390

391 [6] Esposito E, Ravani L, Mariani P *et al.* Curcumin containing monoolein aqueous dispersions: A
392 preformulative study. *Materials Science and Engineering C* 2013; 33: 4923–4934.

393

394 [7] Esposito E, Eblovi N, Rasi S, *et al.* Lipid based supramolecular systems for topical application:
395 a preformulatory study. *AAPS PharmSci* 2003; 5: E30.

396

- 1
2
3 397 [8] Esposito E, Cortesi R, Drechsler M, *et al.* Cubosome Dispersions as Delivery Systems for
4
5 398 Percutaneous Administration of Indomethacin. *Pharm Res* 2005; 22: 2163-73.
6
7 399
8
9 400 [9] Siekmann B, Bunjes H, Koch MHJ *et al.* Preparation and structural investigations of colloidal
10
11 401 dispersions prepared from cubic monoglyceride/water phases. *Int J Pharm* 2002; 244: 33-43.
12
13 402
14
15
16 403 [10] Gustafsson J, Ljusberg-Wharen H, Almgren M, *et al.* Cubic lipid/water phase dispersed into
17
18 404 submicron particles. *Langmuir* 1996; 12: 4611-4613.
19
20
21 405
22
23 406 [11] Worle G, Drechsler M, Koch MHJ, *et al.* Influence of composition and preparation parameters
24
25 407 on the properties of aqueous monoolein dispersions. *Int J Pharm* 2007; 329: 150–157.
26
27 408
28
29 409 [12] Esposito E, Mariani P, Ravani L, *et al.* Nanoparticulate lipid dispersions for bromocriptine
30
31 410 delivery: characterization and in vivo study. *Eur J Pharm Biopharm* 2012; 80: 306-314.
32
33 411
34
35
36 412 [13] Pecora R. Dynamic Light Scattering Measurement of Nanometer Particles in Liquids. *J.*
37
38 413 *Nanoparticle Res* 2000; 2: 123-131.
39
40 414
41
42
43 415 [14] Kligman A M, Christophers E. Preparation of isolated sheets of human stratum corneum. *Arch*
44
45 416 *Dermatol* 1963; 88: 702-705.
46
47 417
48
49 418 [15] Siewert M, Dressman J, Brown C K, *et al.* FIP/AAPS guidelines to dissolution/in vitro release
50
51 419 testing of novel/special dosage forms. *AAPS PharmSciTech* 2003; 4: E7.
52
53
54 420 [16] Sticozzi C, Belmonte G, Pecorelli A, *et al.* Cigarette smoke affects keratinocytes SRB1
55
56 421 expression and localization via H₂O₂ production and HNE protein adducts formation. *PLoS One.*
57
58 422 2012; 7(3): e33592.
59
60

- 1
2
3 423 [17] Golding M, Sein A. Surface rheology of aqueous casein-monoglyceride dispersions. Food
4
5 424 Hydrocoll 2004; 18: 451-461.
6
7 425
8
9
10 426 [18] Zhai J, Waddington L, Wooster T J. *et al.* Revisiting β -casein as a stabilizer for lipid liquid
11
12 427 crystalline nanostructured particles. Langmuir 2011; 27: 14757-14766.
13
14 428
15
16
17 429 [19] Toitou E, Fabin B. Altered skin permeation of highly lipophilic molecule:
18
19 430 Tetrahydrocannabinol. Int J Pharm 1988; 43: 17-22.
20
21 431
22
23
24 432 [20] Shishodia S, Sethi G, Aggarwal B B. Curcumin: getting back to the roots. Ann N Y Acad Sci
25
26 433 2005; 1056: 206–17.
27
28 434
29
30
31 435 [21] Duvoix A, Blasius R, Delhalle S, *et al.* Chemopreventive and therapeutic effects of curcumin.
32
33 436 Cancer Lett 2005; 223: 181–90.
34
35 437
36
37 438 [22] Campbell FC, Collett GP. Chemopreventive properties of curcumin. Future Oncol 2005; 1:
38
39 439 405–14.
40
41 440
42
43
44 441 [23] Singh S, Aggarwal B B. Activation of transcription factor NF-kappa B is suppressed by
45
46 442 curcumin (diferuloylmethane) [corrected]. J Biol Chem 1995; 270: 24995–5000.
47
48 443
49
50
51 444 [24] Chen A, Zheng S. Curcumin inhibits connective tissue growth factor gene expression in
52
53 445 activated hepatic stellate cells in vitro by blocking NF-kappa B and ERK signaling. Br J Pharmacol
54
55 446 2008; 153: 557–567.
56
57 447
58
59
60

- 1
2
3 448 [25] Schon M P, Boehncke W H Psoriasis. N Engl J Med 2005: 352: 1899–1912.
4
5 449
6
7 450 [26] Lindstrom M, Ljusberg-Wahren H, Larsson K *et al.* Aqueous lipid phases of relevance to
8
9 451 intestinal fat digestion and absorption. Lipids 1981:16: 749-754.
10
11 452
12
13 453 [27] Buccheim W, Larsson K. Cubic lipid-protein-water phases. J Colloid Interface Sci 1987: 117:
14
15 454 582-583.
16
17 455
18
19 456 [28] Bodea J C, Kuntsche J, Funari S S, *et al.* Interaction of dispersed cubic phases with blood
20
21 457 components. Int J Pharm 2013: 448: 87-95.
22
23 458
24
25 459 [29] Bronaugh R L, Stewart R F, Simon M, Methods for in vitro percutaneous absorption studies.
26
27 460 VII: Use of excised human skin. J Pharm Sci 1986: 75: 1049-1097.
28
29 461
30
31 462 [30] Ng S F, Rouse J, Sanderson D, *et al.* A comparative study of transmembrane diffusion and
32
33 463 permeation of ibuprofen across synthetic membranes using Franz diffusion cells. Pharmaceutics
34
35 464 2010: 2: 209–223.
36
37 465
38
39 466 [31] Aggarwal B B. Nuclear factor-kappa B: the enemy within. Cancer Cell 2004: 6: 203–208.
40
41 467
42
43 468 [32] Verma IM, Stevenson JK, Schwarz EM, *et al.* Rel/NF- κ B family: intimate tales of association
44
45 469 and disassociation. Genes Dev 1995: 270: 2723–2735.
46
47 470 [33] Takada Y, Singh S, Aggarwal B B. Identification of p65 peptide that selectively inhibits NF-
48
49 471 kappa B activation induced by various inflammatory stimuli and its role in downregulation of NF-
50
51 472 kappaB-mediated gene expression and upregulation of apoptosis. J Biol Chem 2004: 279: 15096–
52
53 473 15104.
54
55
56
57
58
59
60

1
2
3 474

4
5 475 [34] Lallena M J, Diaz-Meco M T, Bren G, *et al.* Activation of IjBa by protein kinase C isoforms.
6
7 476 *Moll Cell Biol* 1999; 19: 2180–2188.

8
9 477

10
11 478 [35] cHuang W C, Chen J J, Chen C C. c-Src dependent tyrosine phosphorylation of IKKbeta is
12
13 479 involved in tumor necrosis factor-alpha-induced intercellular adhesion molecule-1 expression. *J*
14
15 480 *Biol Chem* 2003; 278: 9944– 9952.

16
17
18 481

19
20 482 [36] Yang F, Yamashita J, Tang E, *et al.* The zinc finger C417R of I-kappa B-kinase gamma
21
22 483 impairs lipopolysaccharide and TNF-mediated NF-kappa B activation through inhibiting
23
24 484 phosphorylation of the I-kappa B kinase beta activation loop. *J Immunol* 2004 : 172: 2446–2452.

25
26
27 485

28
29 486 [37] Reddy S, Aggarwal B B. Curcumin is a non-competitive and selective inhibitor of
30
31 487 phosphorylase kinase. *FEBS Lett* 1994; 341: 19–22.

32
33
34 488

35
36 489 [38] Heng M C. Wound healing in adult skin: aiming for perfect regeneration. *Int J Dermatol* 2011:
37
38 490 50(9): 1058-66.

39
40 491
41
42
43
44
45
46
47
48
49
50
51
52
53
54
55
56
57
58
59
60

1
2
3 492 **Figure legends**

4 493

5 494

7 495 **Figure 1.** Cell Viability measured by using cytofluorimetric assay (A) and LDH release (B) in
8 496 HaCaT cells after CUR, NLDs or NLDs+CUR. Triton X represent 100% of LDH release. Data are
9 497 expressed as percentage of control (averages of five independent experiments).
10 498

11 499 **Figure 2.** Cryo-transmission electron microscopy images (cryo-TEM) of NLD stabilized by Na
12 500 cholate and Na caseinate (NLD 3) in the absence (A, B) and in the presence (C, D) of CUR.
13 501

14 502 **Figure 3.** Cryo-transmission electron microscopy images (cryo-TEM) of NLD stabilized by Na
15 503 cholate (NLD 4) in the absence (A) and in the presence (B) of CUR.
16 504

17 505 **Figure 4.** CUR release profiles from CUR-NLD 3 and CUR-NLD 4 obtained by Franz cell
18 506 associated to SCE (A) or nylon membranes (B). Data represent the mean of 4 independent
19 507 experiments \pm S.D.
20 508

21 509 **Figure 5.** Confluent HaCaT cells were scratch wounded, washed and allowed to regenerate from
22 510 scratch wounding in normal conditions (control) or after NLDs+CUR treatment for 24 h and
23 511 photographed. Multiple photographs of the wound were obtained and the distance between the cells
24 512 borders (after wound) represent 0% recovery. Using image analysis Image J software the distance
25 513 calculated in percentage of cellular recovery areas was determined. Data are expressed as
26 514 percentage of 1h (averages of five independent experiments).
27 515

28 516 **Figure 6.** Representative Western blot for Cyclin D1 protein expression after NLDs+CUR
29 517 treatment is showed in the upper panel. Quantification of the Cyclin D1 bands is shown in the
30 518 bottom panel. Data are expressed as arbitrary units (averages of five independent experiments, *p <
31 519 0.05). β -actin was used as loading control.
32 520

33 521 **Figure 7.** Immunofluorescence of HaCaT cells after NLDs+CUR treatment for 1h showed the
34 522 localization of NF- κ B (p65 subunit, green). Images are merged and representative of at least 100
35 523 cells viewed in each experiments (n = 5). Nuclei (blue) were stained with DAPI. Original
36 524 Magnification X 630.
37 525

38 526

39 527

40 528

41 529

42

43

44

45

46

47

48

49

50

51

52

53

54

55

56

57

58

59

60

530
531**Table I.** Composition of NLD

Component (% w/w)	NLD 1	NLD 2	NLD 3	NLD 4
Monooleine	4.5	4.5	4.5	4.5
Poloxamer 407	0.5	0.5	-	-
Na Cholate	0.15	-	0.15	0.15
Na caseinate	-	-	0.07	-
H₂O	94.85	95	95.28	95.35

^aIn the case of drug containing NLD, curcumin content was 0.015 %

532
533
534
535
536

537

Table II. Size distribution parameters of NLD, as determined by PCS.

Dimensional parameter		
Formulation	Intensity mean diameter (nm)	Polydispersity Index
NLD 1	154.5	0.29
NLD 2	198.9	0.26
NLD 3	227.5	0.28
NLD 4	189.8	0.27

PCS data are means of 5 determinations on different batches of the same type of dispersion, SD was always comprised between $\pm 5\%$

538

539

540

541

542

Table III. PCS parameters of NLD 3 and 4 in the presence of CUR.

543

Parameter	NLD 3	NLD 3 CUR	NLD 4	NLD 4 CUR
Z-Average (nm)	227.20	218.38	210.70	206.80
P.I.	0.23	0.29	0.23	0.27

CUR denotes the formulation produced in the presence of curcumin; PI: Poldispersity Index.

PCS data are means of 5 determinations on different batches of the same type of dispersion, SD was always comprised between $\pm 5\%$

544

545

546

547

548

549

550

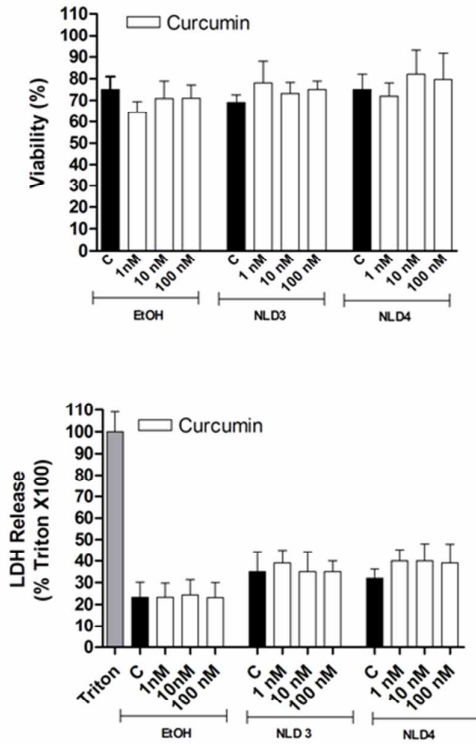
551

552

553

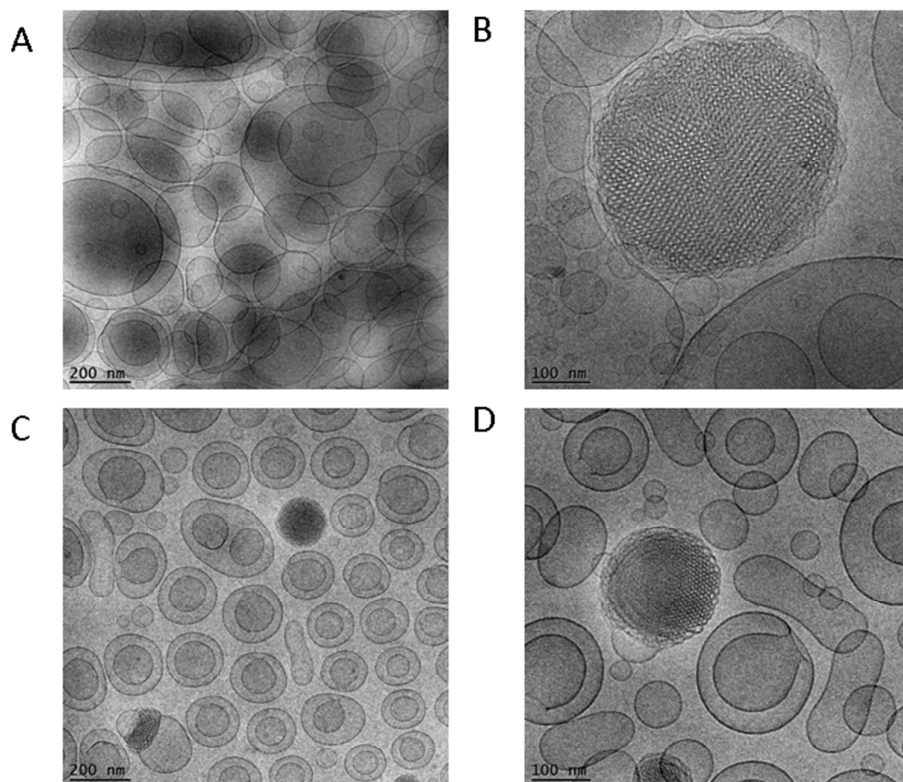
554

Fig. 1



555
556
557
558
559

Fig. 2



560

561

562

563

564

565

566

567

568

569

570

571

572

573

574

575

576

577

578

579

580

581

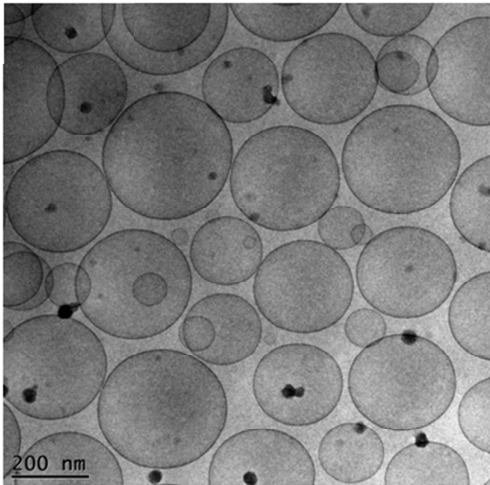
582

583

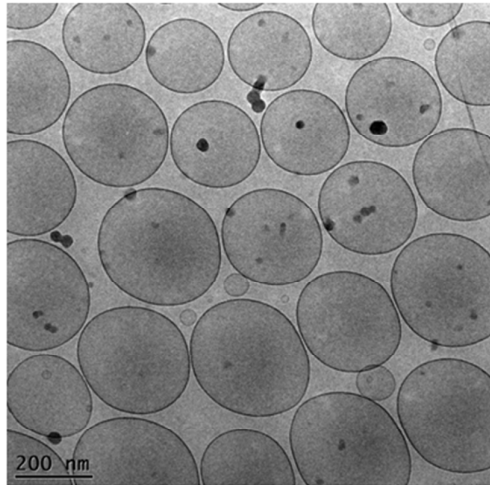
584

Fig. 3

A



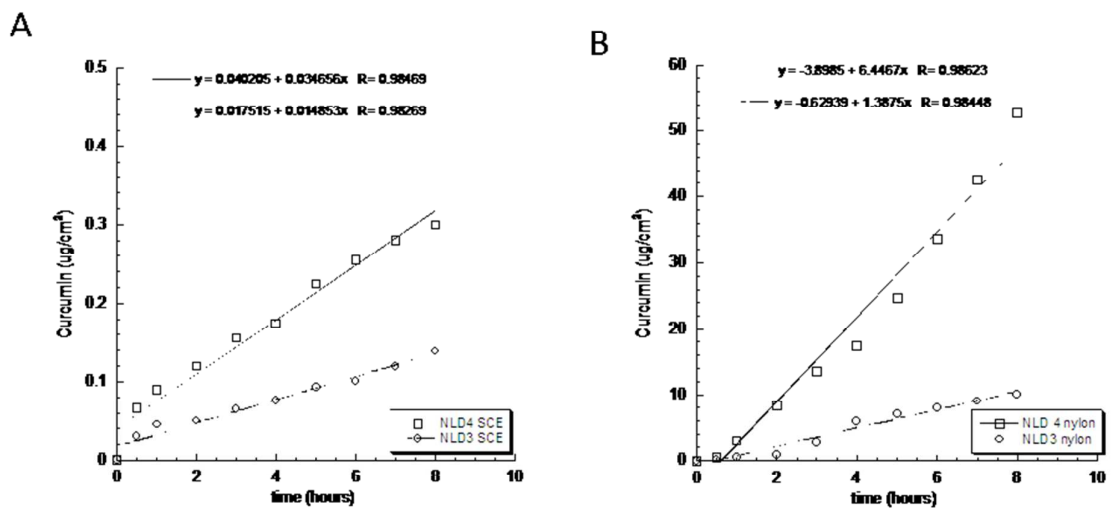
B



585
586
587
588
589
590
591
592
593
594
595
596
597
598
599
600
601
602
603
604
605
606
607
608
609
610

ew Only

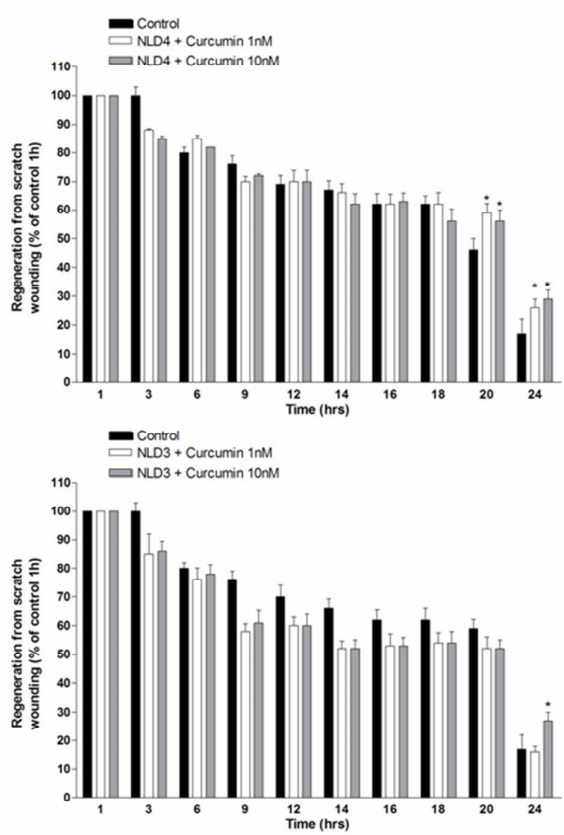
Fig. 4



611
612
613
614
615
616
617
618
619
620
621
622
623
624
625
626
627
628
629
630
631
632
633
634
635
636
637

1
2
3 638
4
5
6
7
8
9
10
11
12
13
14
15
16
17
18
19
20
21
22
23
24
25
26
27
28
29
30
31
32
33

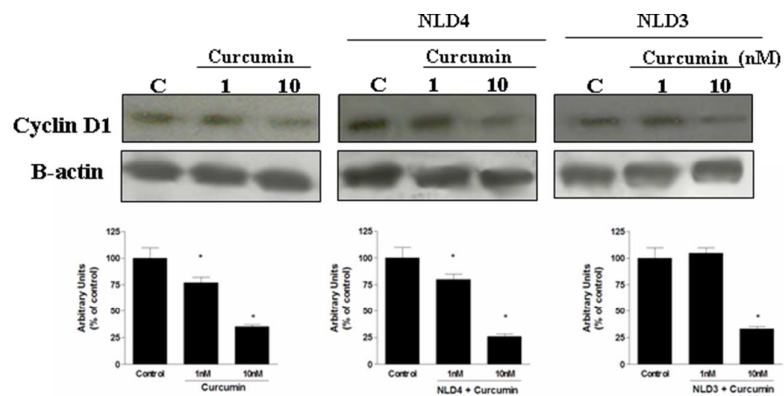
Fig. 5



34 639
35 640
36 641
37 642
38 643
39 644
40 645
41 646
42 647
43 648
44 649
45 650
46 651
47 652
48 653
49 654
50 655
51 656
52 657
53 658
54 659
55 660
56 661
57
58
59
60

662
663

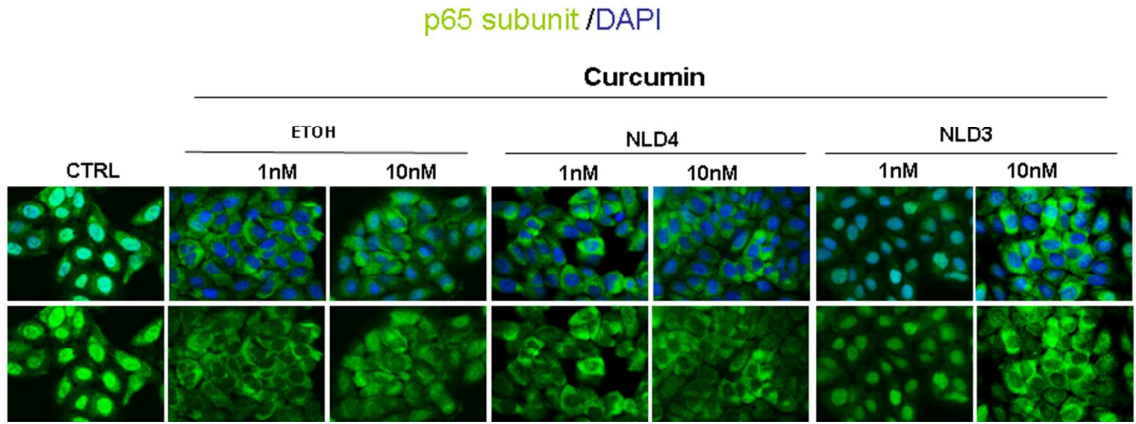
Fig. 6

664
665
666
667
668
669
670
671
672
673
674
675
676
677
678
679
680
681
682
683
684
685
686
687
688

1
2
3
4
5
6
7
8
9
10
11
12
13
14
15
16
17
18
19
20
21
22
23
24
25
26
27
28
29
30
31
32
33
34
35
36
37
38
39
40
41
42
43
44
45
46
47
48
49
50
51
52
53
54
55
56
57
58
59
60

689

Fig. 7



690

AW Only